inorganics

MDPI

Article

Thionitrosyl Complexes of Rhenium and Technetium with PPh_3 and Chelating Ligands—Synthesis and Reactivity

Domenik Nowak, Adelheid Hagenbach, Till Erik Sawallisch and Ulrich Abram *

Institute of Chemistry and Biochemistry, Freie Universität Berlin, Fabeckstr. 34/36, D-14195 Berlin, Germany
* Correspondence: ulrich.abram@fu-berlin.de

Abstract: In contrast to corresponding nitrosyl compounds, thionitrosyl complexes of rhenium and technetium are rare. Synthetic access to the thionitrosyl core is possible by two main approaches: (i) the treatment of corresponding nitrido complexes with S_2Cl_2 and (ii) by reaction of halide complexes with trithiazyl chloride. The first synthetic route was applied for the synthesis of novel rhenium and technetium thionitrosyls with the metals in their oxidation states "+1" and "+2". $[M^{V}NCl_2(PPh_3)_2]$, $[M^{V}NCl(PPh_3)(L^{OMe})]$ and $[M^{VI}NCl_2(L^{OMe})]$ (M = Re, Tc; $\{L^{OMe}\}^-$ = (η^5-cyclopentadienyl)tris(dimethyl phosphito-*P*)cobaltate(III)) complexes have been used as starting materials for the synthesis of $[Re^{II}(NS)Cl_3(PPh_3)_2]$ (**1**), $[Re^{II}(NS)Cl_3(PPh_3)(OPPh_3)]$ (**2**), $[Re^{II}(NS)Cl(PPh_3)(L^{OMe})]^+$ (**4a**), $[Re^{II}(NS)Cl_2(L^{OMe})]$ (**5a**), $[Tc^{II}(NS)Cl(PPh_3)(L^{OMe})]^+$ (**4b**) and $[Tc^{II}(NS)Cl_2(L^{OMe})]$ (**5b**). The triphenylphosphine complex **1** is partially suitable as a precursor for ongoing ligand exchange reactions and has been used for the synthesis of $[Re^{I}(NS)(PPh_3)(Et_2btu)_2]$ (**3a**) (HEt_2btu = *N*,*N*-diethyl-*N*′-benzoyl thiourea) containing two chelating benzoyl thioureato ligands. The novel compounds have been isolated in crystalline form and studied by X-ray diffraction and spectroscopic methods including IR, NMR and EPR spectroscopy and (where possible) mass spectrometry. A comparison of structurally related rhenium and technetium complexes allows for conclusions about similarities and differences in stability, reaction kinetics and redox behavior between these *4d* and *5d* transition metals.

Keywords: rhenium; technetium; thionitrosyl complexes; synthesis; X-ray diffraction; EPR; NMR

Citation: Nowak, D.; Hagenbach, A.; Sawallisch, T.E.; Abram, U. Thionitrosyl Complexes of Rhenium and Technetium with PPh_3 and Chelating Ligands—Synthesis and Reactivity. *Inorganics* **2024**, *12*, 210. https://doi.org/10.3390/inorganics12080210

Academic Editors: Wolfgang Linert, Sunčica Roca and Monika Kovačević

Received: 10 July 2024
Revised: 25 July 2024
Accepted: 26 July 2024
Published: 31 July 2024

1. Introduction

The two "group 7" elements technetium and rhenium possess radioactive isotopes (^{99m}Tc, ^{186,188}Re), which make them more than interesting for nuclear medical applications [1–11]. The metastable nuclide ^{99m}Tc (pure γ-emitter, half-life 6 h, γ-energy: 411 keV) is sometimes denoted as the "workhorse" of diagnostic nuclear medicine, since more than 80 percent of clinical applications in this field in more than 10,000 hospitals worldwide are performed with ^{99m}Tc-containg pharmaceuticals [12]. This dominating position is mainly due to the favorable nuclear properties of this nuclide: (i) an almost optimal γ-energy without considerable amounts of accompanying particle radiation, (ii) a half-life which is long enough to examine metabolic processes but short enough to avoid a considerable radiation burden to the patient and (iii) the formation of ^{99m}Tc in a so-called generator system from ^{99}Mo [13], which ensures a permanent availability of this nuclide in the clinics. A similar generator system starting from ^{188}W as mother nuclide is also available for the supply of ^{188}Re ($E_{\beta,max}$: 2.12 MeV, $E_{\beta,av}$: 784 keV, half-life: 16.9 h), a beta-emitting isotope with potential in nuclear medical therapy [14]. For both isotopes, kit-like preparations of the pharmaceuticals have been developed, which allow for a rapid and cost-efficient production of the individual administrations [1,14].

^{99m}Tc and ^{188}Re are also under discussion as an almost perfect example of a "matched pair" of nuclides for theragnostic applications [15,16], which is a modern approach in personalized medicine, where an optimized dosage of a therapeutic drug becomes possible by the parallel monitoring of the therapeutic effects by a diagnostic counterpart.

Although the syntheses of ^{99m}Tc and ^{188}Re compounds proceed at an approximate nanomolar level due to the low (chemical) concentrations obtained from the corresponding nuclide generators, fundamental chemical and structural studies concerning the formed compounds are commonly conducted with natural rhenium and the long-lived technetium isotope ^{99}Tc, a weak beta emitter (E_{max} = 297 keV, half-life 2.11 × 10^5 years), which is also available in macroscopic amounts. During such studies, occasionally at the first glance, unusual solutions for the development of novel radiopharmaceuticals have been found, including several organometallic approaches [17–23] and drugs on the basis of nitrido [24–27] or hydrazido compounds [28–30]. Finally, the usability of a potential solution is decided by the successful transfer to the low concentration level of ^{99m}Tc and the stability of the product under aqueous conditions. Consequently, the potential of a chemical solution for a final medical application cannot easily be predicted by a simple, intuitive evaluation of a substance or a substance class. A good example is "^{99m}Tc-sestamibi", a cationic organotechnetium(I) complex with six isocyanide ligands. As a compound with six technetium-carbon bonds, it was most probably not in the first row for candidates for myocardial imaging. Nowadays, it is one of the most used radiopharmaceuticals worldwide and, up to now, more than 40 million patients have been examined with this drug [17]. Also, nitrosyl complexes of technetium were considered for such purposes and related ^{99m}Tc compounds have been tested for their biodistribution [31]. The related structural chemistry was performed with the long-lived isotope ^{99}Tc and starting from these early days in the 1980s, our knowledge about nitrosyltechnetium compounds has significantly increased.

In contrast to the relatively large number of nitrosyl complexes of the elements rhenium [32–40] and technetium [40–60], there are only a few reports about thionitrosyls of these two elements [61–80]. This should be mainly due to the lack of a readily available monomeric nitrogen sulfide. Although the thionitrosyl radical has been described spectroscopically and some NS^+ salts have been isolated [81–84], the synthesis of such compounds remains a challenge and they have only occasionally been used as precursors for the synthesis of thionitrosyl complexes [61,83,84]. More convenient are reactions starting from cyclic compounds such as tetrasulfur tetranitride, S_4N_4, or trithiazyltrichloride, $(NSCl)_3$ (Figure 1), which readily undergo thermal or photochemical decomposition under release of NS^+ or $NSCl^+$ building blocks. But it should be noted that N_4S_4 is a potentially dangerous compound, which tends to explode on heating or upon shock. Thus, it is not a favored agent at least for reactions with the radioactive technetium. Finally, the most promising synthetic approach to thionitrosyl complexes is the addition of a "sulfur atom" to a nitrido ligand. A variety of "sulfur sources" have been used including elemental sulfur, $SOCl_2$, dithionite or NCS^- ligands. Most successful, however, are reactions of nitrido complexes with S_2Cl_2, which give low-valent thionitrosyl species in good yields. About reactions following the latter approach, we report in the present paper starting from different rhenium and technetium complexes with the metals in the oxidation states "+5" or "+6".

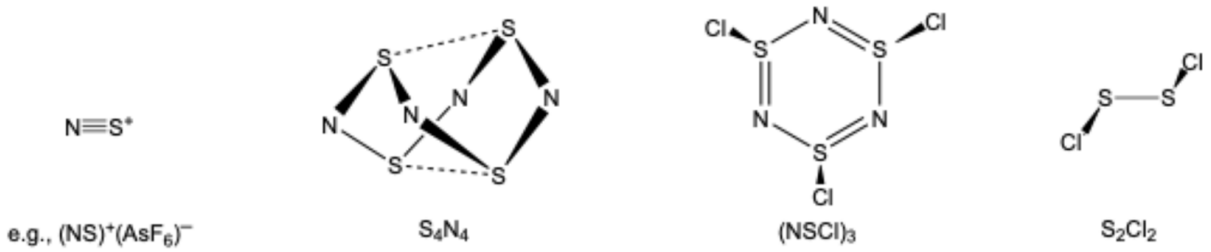

Figure 1. Common starting materials for the synthesis of thionitrosyl complexes.

2. Results and Discussion

2.1. Triphenylphosphine Complexes

Treatment of the rhenium(V) complex $[ReNCl_2(PPh_3)_2]$ with an excess of disulfur dichloride in refluxing dichloromethane results in a subsequent dissolution of the sparingly soluble starting material and a dark-red, almost black solution is formed, from which the thionitrosyl complexes $[Re(NS)Cl_3(PPh_3)_2]$ (**1**) and $[Re(NS)Cl_3(PPh_3)(OPPh_3)]$ (**2**) can be isolated. The parallel formation of phosphine and phosphine oxide complexes is not completely surprising with respect to the oxidizing conditions in the reaction mixture and has been observed previously during similar reactions with $[TcNCl_2(PMe_2Ph)_3]$ [74]. The two products can readily be separated during the crystallization procedure since compound **2** is highly soluble in acetone, while complex **1** is almost insoluble in this solvent. During the slow evaporation of CH_2Cl_2/acetone solutions of mixtures of **1** and **2**, $[Re(NS)Cl_3(PPh_3)_2]$ precipitates first as dark-red crystals, while the orange-yellow crystals of **2** do not deposit until almost all acetone is evaporated. The best method for the isolation of pure $[Re(NS)Cl_3(PPh_3)_2]$, however, is the addition of an excess of PPh_3 during the synthesis, which obviously avoids the formation of significant amounts of the phosphine oxide complex (Scheme 1).

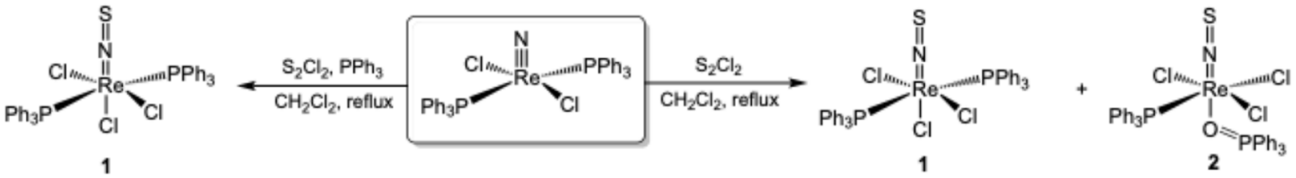

Scheme 1. Syntheses of $[Re(NS)Cl_3(PPh_3)_2]$ (**1**) and $[Re(NS)Cl_3(PPh_3)(OPPh_3)]$ (**2**).

The infrared spectra of the complexes show the characteristic $\nu_{(NS)}$ stretches at 1213 cm^{-1} (phosphine complex) and 1230 cm^{-1} (phosphine oxide complex). These values are in agreement with such recorded for other rhenium complexes and those calculated for similar chromium(I) species [62]. The difference of approximately 20 cm^{-1} reflects a stronger back-donation in compound **1** compared with **2**. Since the oxidation state of rhenium in both compounds is "+2", the observed difference indicates some changes in the coordination sphere of the transition metal. Particularly the electronic properties of the ligand in the *trans* position to the thionitrosyl ligand have a direct influence to the donor/acceptor behavior of NS^+.

Single-crystal X-ray diffraction confirms that the oxidation of one of the PPh_3 ligands is accompanied with a ligand rearrangement and the $OPPh_3$ ligand in **2** occupies the position *trans* to NS^+ instead of Cl^- in **1**. The molecular structures of both complexes are depicted in Figure 2 and selected bond lengths and angles are summarized in Table 1. It becomes evident that the thionitrosyl units are arranged linearly in both compounds with Re–N–S angles between 167° and 178°. Such a bonding situation has been found for all hitherto structurally characterized thionitrosyl complexes. Also, the direction of a formed phosphine oxide ligand in the *trans* position to a multiply bonded ligand is not without precedence and has been observed before during the formation of $[Tc(NS)Cl_3(PMe_2Ph)(OPMe_2Ph)$ from *cis,mer*-$[TcNCl_2(PMe_2Ph)_3]$ [74]. More generally, the presence of one triphenylphosphine oxide ligand in the coordination sphere of a transition metal favors the *cis* coordination to PPh_3, since the steric and electronic effects, which direct two PPh_3 ligands commonly into *trans* positions to each other, are significantly lowered.

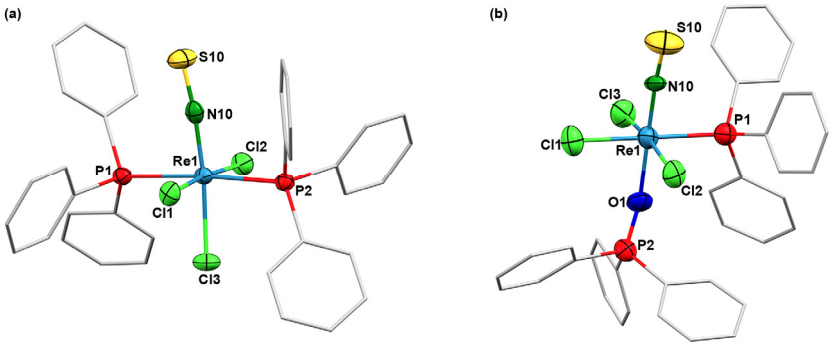

Figure 2. Molecular structures of (**a**) [Re(NS)Cl_3(PPh_3)$_2$] (**1**) and (**b**) [Re(NS)Cl_3(PPh_3)($OPPh_3$)] (**2**). Thermal ellipsoids represent 50 percent probability.

Table 1. Selected bond lengths (Å) and angles (°) in [Re(NS)Cl_3(PPh_3)$_2$] (**1**) and (b) [Re(NS)Cl_3(PPh_3)($OPPh_3$)] (**2**).

	Re1–N10	N10–S10	Re1–Cl1	Re1–Cl2	Re1–Cl3	Re1–P1	Re1–P2/O1	O1–P2	Re1–N10–S10	Re1–O1–P2
1	1.795(5)	1.518(5)	2.353(1)	2.340(1)	2.416(1)	2.540(2)	2.555(2)	-	174.4(3)	-
2 [(1)]	1.77(1) 1.77(1)	1.53(1) 1.52(1)	2.368(4) 2.357(4)	2.255(3) 2.332(3)	2.338(3) 2.366(3)	2.506(4) 2.584(4)	2.100(8) 2.099(8)	1.509(9) 1.497(9)	167.2(7) 178.4(6)	155.7(6) 164.5(5)

[(1)] Values for two crystallographically independent molecules.

[Re(NS)Cl_3(PPh_3)$_2$] (**1**) as well as [Re(NS)Cl_3(PPh_3)($OPPh_3$)] (**2**) contain rhenium in the oxidation state "+2". Due to the corresponding $5d^5$ "low spin" configuration, they are paramagnetic with one unpaired electron. This allows for the detection of resolved EPR spectra in solution. Figure 3 shows the spectra of both compounds at various temperatures. The spectra in liquid solutions (Figure 3a) consist of six hyperfine lines due to interactions of the unpaired electron with ^{185,187}Re, both having a nuclear spin of I = 5/2. Superhyperfine couplings due to interactions of the unpaired electron with the coordinating ^{31}P (I = 1/2), ^{35,37}Cl (I = 3/2) or ^{14}N (I = 1) nuclei could not be resolved. The frozen solution EPR spectra, which are shown in Figure 3b, confirm the presence of essentially axially symmetric, randomly oriented S = ½ spin systems with resolved parallel and perpendicular sets of ^{185,187}Re hyperfine lines. The analysis of the spectral parameters indicates the presence of a small rhombic component in the perpendicular part of the spectrum of complex **1**, which has been taken into account during the simulation. The simulated spectra, which have been used to derive the spectral parameters, are depicted in the Supporting Material.

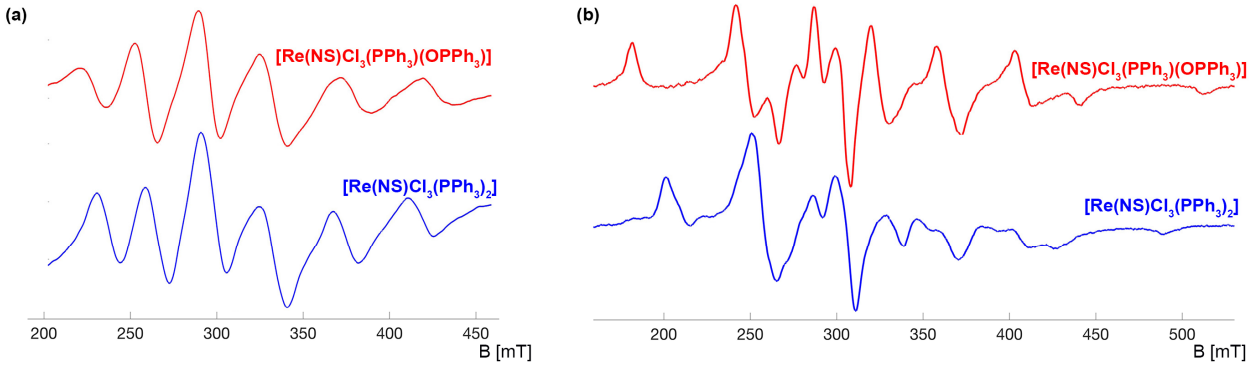

Figure 3. X-band EPR spectra of **1** and **2**: (**a**) at room temperature (parameters for **1** in CH_2Cl_2: $g_0 = 2.025$; $a_0^{Re} = 342 \times 10^{-4}$ cm^{-1}; parameters for **2** in acetone: $g_0 = 2.017$; $a_0^{Re} = 372 \times 10^{-4}$ cm^{-1}) and (**b**) in frozen solution at T = 77 K (parameters for **1** in CH_2Cl_2: $g_x = 2.110$, $g_y = 1.991$, $g_z = 1.943$; $A_x^{Re} = 281 \times 10^{-4}$ cm^{-1}, $A_y^{Re} = 283 \times 10^{-4}$ cm^{-1}, $A_z^{Re} = 524 \times 10^{-4}$ cm^{-1}; parameters for **2** in acetone: $g_{\|} = 1.923$, $g_{\perp} = 2.008$; $A_{\|}^{Re} = 594 \times 10^{-4}$ cm^{-1}, $A_{\perp}^{Re} = 293 \times 10^{-4}$ cm^{-1}).

As already mentioned, couplings with the ^{31}P nuclei of the coordinated phosphine ligands could not be resolved in the spectra of **1** and **2**. This finding is in contrast to the previously studied technetium(II) complexes $[Tc(NS)Cl_3(PMe_2Ph)_2]$ and $[Tc(NS)Cl_3(PMe_2Ph)(OPMe_2Ph)]$, where the ^{99}Tc hyperfine signals of the parallel part show splittings into triplets (phosphine complex) or doublets (phosphine/phosphine oxide complex) and provide direct information for the occupation of their respective equatorial coordination spheres [74,77,85,86]. The larger line-widths of the EPR spectra obtained for the rhenium complexes prevent the resolutions of such couplings. Nevertheless, a remarkable trend in the EPR spectral parameters should be mentioned: the isotropic $^{185,187}Re$ coupling constants a_0^{Re} show a dependence on the number of chlorido ligands in the equatorial coordination sphere in a way that they increase from compound **1** ($2\ Cl^-$: 342×10^{-4} cm^{-1}) via compound **2** ($3\ Cl^-$: 372×10^{-4} cm^{-1}) to the $[Re(NS)Cl_4]^-$ anion ($4\ Cl^-$: 457×10^{-4} cm^{-1} [66]). In the same sequence of complexes, the corresponding g_0 values decrease. Similar trends are also observed for the *g* values and coupling constants of the anisotropic spectra, which reflects considerable changes in the MO of the unpaired electron mainly due to the presence or absence of phosphine ligands.

2.2. Complexes with Chelating Ligands

Since the triphenylphosphine complexes **1** and **2** might have potential as precursors for the synthesis of more thionitrosyl complexes of rhenium, we tested some ligand exchange reactions with the chelating ligands shown in Figure 4. HEt_2btu is a potentially bidentate chelator. It readily deprotonates after the addition of a supporting base and stable complexes are known with almost all common transition metals. This also includes rhenium and technetium complexes with the metals in several oxidation states [87–94]. The tripodal, organometallic ligand $\{L^{OMe}\}^-$ belongs to a classical family of tripodal ligands, which has been designed by Wolfgang Kläui and tested for a plethora of various applications [95,96]. Also, a number of rhenium complexes with this ligand are known and it is the first example of a chelating ligand, which forms stable technetium complexes with the metal in seven different oxidation states [54,95–101].

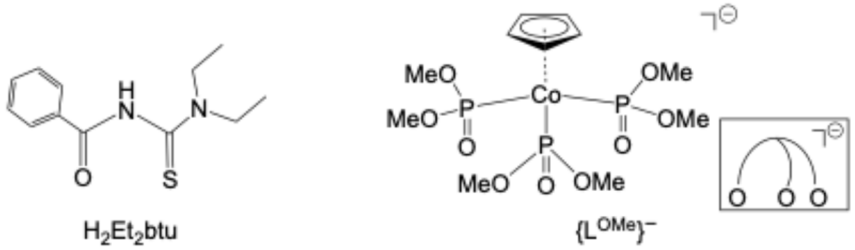

H_2Et_2btu $\{L^{OMe}\}^-$

Figure 4. *N*,*N*-Diethyl-*N*′-benzoylthiourea (HEt_2btu) and (η^5-cyclopentadienyl)tris(dimethyl phosphito-P) cobaltate(III) ($\{L^{OMe}\}^-$) as typical chelating ligands for ligand exchange reactions.

Reactions of $[Re(NS)Cl_3(PPh_3)_2]$ with HEt_2btu in a mixture of CH_2Cl_2 and EtOH proceeded at room temperature (Scheme 2). After the addition of a small amount of Et_3N as a supporting base, the red reaction mixture immediately turned dark brown and a red-brown solid could be isolated. Single crystals suitable for X-ray diffraction were obtained by the slow evaporation of a CH_2Cl_2 solution. The deprotonation of HEt_2btu and its coordination as an *S*,*O* chelate is strongly indicated by the IR spectrum of the product by the disappearance of the NH stretches of the ligands and a strong bathochromic shift of the $\nu_{C=O}$ band by almost 200 cm^{-1}. This is typical for chelate-bonded R_2btu^- ligands [87]. Reduction of the metal ion is frequently observed during reactions with sulfur-containing ligands and, thus, the product of the described reaction with HEt_2btu is the diamagnetic rhenium(I) complex $[Re(NS)(PPh_3)(Et_2btu)_2]$ (**3a**). This allows for the measurement of NMR spectra. They support the composition of the product as is performed by the mass spectrum.

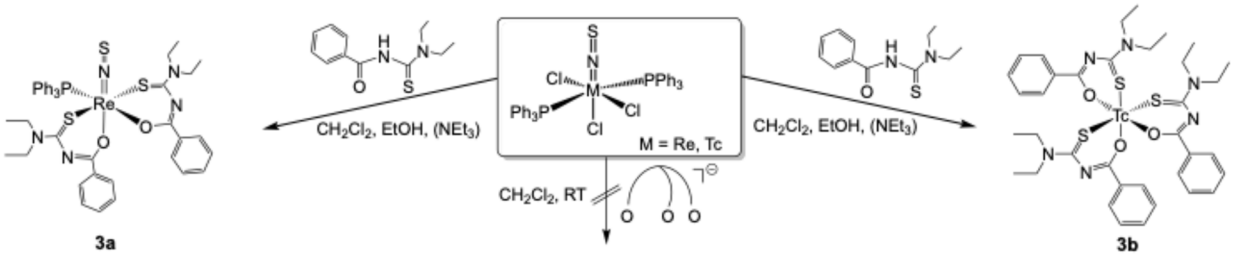

Scheme 2. Ligand exchange reactions starting from $[Re(NS)Cl_3(PPh_3)_2]$ (**1**).

The results of the spectroscopic studies are confirmed by a single-crystal structure analysis of the product. Figure 5 depicts the molecular structure of compound **3a**, which shows the expected linear arrangement of the thionitrosyl ligand (Table 2). The equatorial coordination sphere of rhenium is occupied by an *S*,*O* chelate, a PPh_3 and the sulfur atom of the second Et_2btu^- ligand. Interestingly, the two Re–O single bonds are almost equal, which indicates similar structural *trans* influences induced by the NS^+ and the PPh_3 ligands. The N–S distance in the rhenium(I) complex is markedly longer than in the rhenium(II) complexes **1** and **2**, which might be a consequence of a stronger back-donation of the d^6 metal ion into anti-bonding orbitals of the thionitrosyl ligand. Unfortunately, the corresponding IR stretch, which is normally more indicative, cannot be assigned unambiguously for **3a** due to many overlapping bands in the respective range of the spectrum.

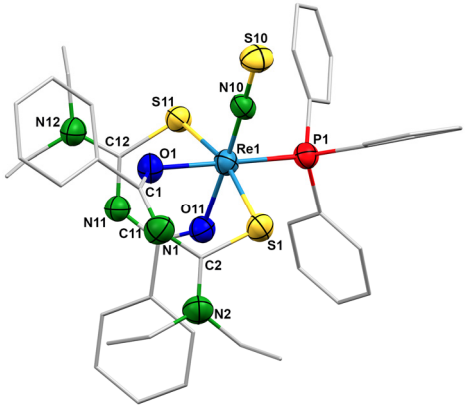

Figure 5. Molecular structure of $[Re(NS)(PPh_3)(Et_2btu)_2]$ (**3a**). Thermal ellipsoids represent 50 percent probability.

Table 2. Selected bond lengths (Å) and angles (°) $[Re(NS)(PPh_3)(Et_2btu)_2]$ (**3a**).

Re1–N10	N10–S10	Re1–P1	Re1–S1	Re1–O1	Re1–S11	Re1–O11	O1–C1	C1–N1	N1–C2
1.749(4)	1.571(4)	2.362(1)	2.401(1)	2.101(3)	2.439(1)	2.103(4)	1.296(6)	1.301(7)	1.353(7)
C2–N2	C2–S1	O11–C11	C11–N11	N11–C12	C12–N12	C12–S11		Re1–N10–S10	
1.319(7)	1.755(6)	1.266(6)	1.329(6)	1.338(7)	1.325(7)	1.758(6)		176.5(3)	

With respect to the clean reaction of $[Re(NS)Cl_3(PPh_3)_2]$ with HEt_2btu and the ready formation of the thionitrosylrhenium(I) complex **3a**, a surprising result was obtained for an analogous reaction of the corresponding technetium complex $[Tc(NS)Cl_3(PPh_3)_2]$. It proceeded under complete removal of the NS^+ ligand and oxidation of the metal ion. The resulting technetium(III) tris complex $[Tc(Et_2btu)_3]$ (Scheme 2) has been reported before (i) as the product of the direct reduction of pertechnetate with $SnCl_2$ in the presence of excess ligand [102], and (ii) by a subsequent reduction/ligand exchange procedure starting from $(NBu_4)[TcOCl_4]$ [87]. The observed lability of the thionitrosyl unit is a considerable drawback for a potential use of **1** as precursor in ligand exchange procedures and is accom-

panied by another disappointing experience during attempted reactions with Na{L^{OMe}}. Although reactions of an entire series of different technetium and rhenium complexes with the "Kläui ligand" give well-defined and stable products [95–101], attempted reactions with **1** at room temperature did not proceed. Heating of such reaction mixtures finally gave a small amount of the chelate [Re(NS)Cl(PPh_3)(L^{OMe})], but the yield was low and the product was accompanied by a number of side-products and impurities, which precluded the isolation of a pure compound in reasonable yields. Consequently, we preferred the second general approach to thionitrosyl compounds: the reaction of nitrido complexes with S_2Cl_2. Corresponding starting materials with $\{L^{OMe}\}^-$ ligands, [MNCl(PPh_3)(L^{OMe})] and [MNCl_2(L^{OMe})] complexes with M = Re or Tc, are readily available from simple procedures, and the reactions with S_2Cl_2 (Scheme 3) give the products [M(NS)Cl(PPh_3)(L^{OMe})]Cl (M = Re: **4a**; M = Tc: **4b**) and [M(NS)Cl_2(L^{OMe})] (M = Re: **5a**; M = Tc: **5b**) in reasonable yields and good purities.

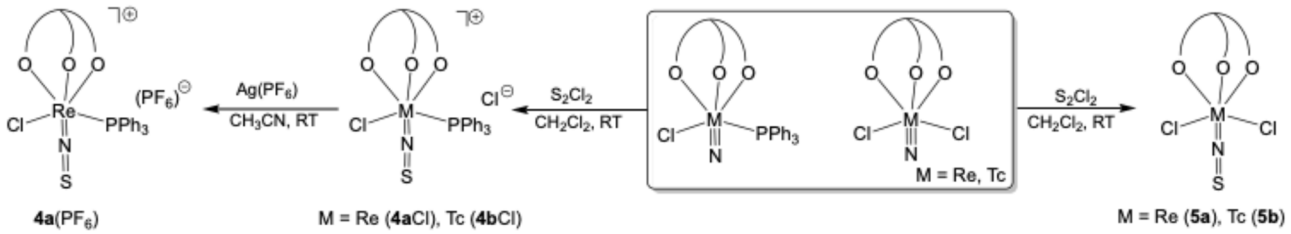

Scheme 3. Formation of thionitrosyl complexes containing the "Kläui ligand" $\{L^{OMe}\}^-$.

The reactions with all four starting complexes are restricted to the nitrido ligands and the remaining coordination spheres of the metals remain unchanged. Cationic thionitrosyls of rhenium(II) and technetium(II) are formed, when [M^{V}NCl(PPh_3)(L^{OMe})] complexes (M = Re, Tc) are used as precursors. The products can be precipitated from the reaction mixture as yellow (Re compound, **4a**Cl) and red (Tc complex, **4b**Cl) chloride salts by the addition of *n*-hexane. Microcrystalline samples were obtained after recrystallization of CH_2Cl_2/*n*-hexane mixtures. For the rhenium complex, the PF_6^- salt was prepared by metathesis with $AgPF_6$. Orange-yellow needles of [Re(NS)Cl(PPh_3)(L^{OMe})](PF_6), **4a**(PF_6), were suitable for X-ray diffraction. The structure of the complex cation is shown in Figure 6a and selected bond lengths and angles are summarized in Table 3. Expectedly, the $\{L^{OMe}\}^-$ ligands act as tripods in both complexes, which directs the remaining three ligands into *trans* positions of their oxygen atoms. The M–N–S angles are close to 180° in both compounds.

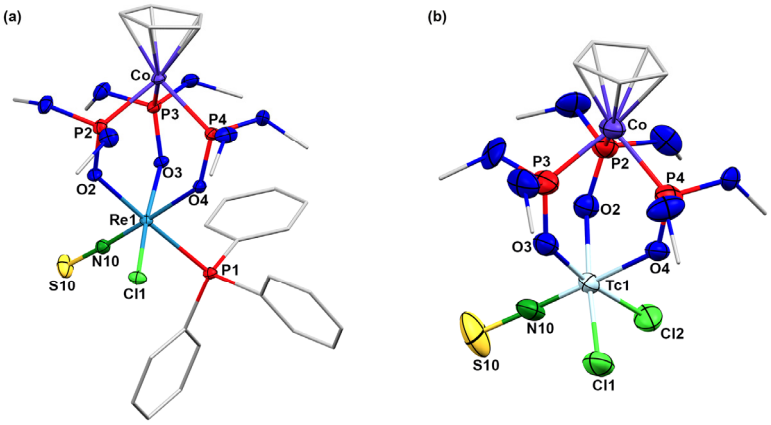

Figure 6. Molecular structures of (**a**) the complex cation of [Re(NS)Cl(PPh_3)(L^{OMe})](PF_6) (**4a**) and (**b**) [Tc(NS)Cl_2(L^{OMe})] (**5b**). Thermal ellipsoids represent 50 percent probability.

Table 3. Selected bond lengths (Å) and angles (°) in [Re(NS)Cl(PPh$_3$)(L^{OMe})](PF$_6$) (**4a**(PF$_6$)) and (b) [Tc(NS)Cl$_2$(L^{OMe})] (**5b**).

	M1–N10	N10–S10	M1–Cl1	M1–Cl2	M1–P1	M1–O2	M1–O3	M1–O4	M1–N10–S10
4a	1.752(5)	1.554(5)	2.337(1)	-	2.475(1)	2.071(3)	2.032(3)	2.083(3)	175.4(3)
5b [(1)]	1.732(7) 1.75(1)	1.540(7) 1.54(1)	2.339(3) 2.330(3)	2.343(2) 2.344(3)	-	2.060(6) 2.068(5)	2.047(6) 2.057(6)	2.095(5) 2.088(5)	171.7(6) 172.0(8)

[(1)] Values for two crystallographically independent molecules.

Similar reaction patterns are observed for [ReNCl$_2$((L^{OMe})] and [TcNCl$_2$((L^{OMe})]. Both precursors contain the transition metals in their oxidation states "+6", while the products [Re(NS)Cl$_2$(L^{OMe})] (**5a**) and [Tc(NS)Cl$_2$(L^{OMe})] (**5b**) are Re(II) and Tc(II) complexes (Scheme 3). An X-ray crystal structure determination has been performed for the technetium complex and its molecular structure is shown in Figure 6b. The general structural features found for the cation **4a** also apply to technetium complex **5b** (Table 3).

As compounds **1** and **2**, the {L^{OMe}}$^-$ complexes of the present study, are paramagnetic with a d^5 "low spin" configuration, this results in S = ½ spin systems and allows us to record resolved EPR spectra in liquid and frozen solutions. The spectra have essentially axial symmetry with well-resolved ^{185,187}Re and ^{99}Tc hyperfine couplings in their parallel and perpendicular parts. Figure 7 shows exemplarily the spectra obtained for [Tc(NS)Cl(PPh$_3$)(L^{OMe})]Cl (**4b**Cl).

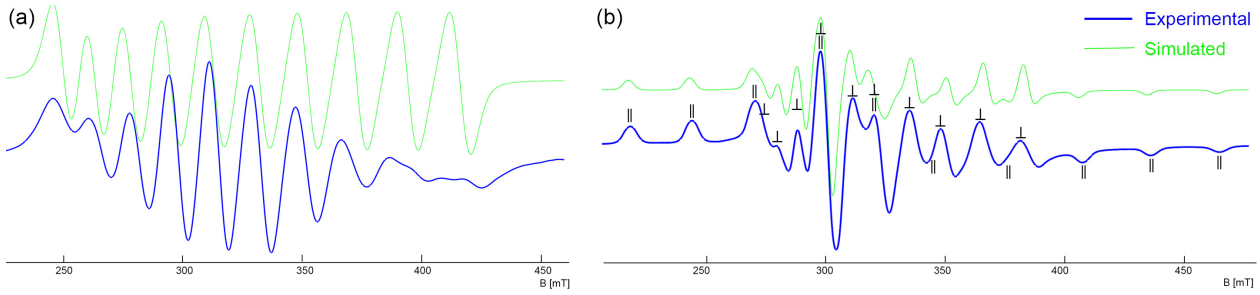

Figure 7. Liquid solution EPR spectra of [Tc(NS)Cl(PPh$_3$)(L^{OMe})] in CH$_2$Cl$_2$ (**a**) at room temperature and (**b**) at T = 77 K (assignment of the ^{99}Tc lines to the parallel and perpendicular parts of the spectrum is indicated).

^{99}Tc has a nuclear spin of I = 9/2, which results in a ten-line pattern in the spectrum in liquid solution, while two sets of ten ^{99}Tc hyperfine lines (each one in the parallel and one in the perpendicular part of the spectrum) are characteristic for the anisotropic frozen-solution spectrum as can be described by the Spin Hamiltonian (1), where $g_{\|}$, $g_{\perp}$, $A_{\|}{}^{M.}$ and $A_{\perp}{}^{M}$ are the principal values of the ^{99}Tc and ^{185,187}Re hyperfine tensors A^M. The spectral parameters are summarized in Table 4.

$$\hat{H}_{sp} = \beta_e \left[g_{\|} B_z \hat{S}_z + g_{\perp} \left(B_x \hat{S}_x + B_y \hat{S}_y \right) \right] + A_{\|}^{M} \hat{S}_z \hat{I}_z + A_{\perp}^{M} \left(\hat{S}_x \hat{I}_x + \hat{S}_y \hat{I}_y \right) \quad (1)$$

Table 4. EPR parameters of the Re(II) and Tc(II) complexes with {L^{OMe}}$^-$ ligands, coupling constants are given in 10^{-4} cm^{-1}.

	g_0	$a_0{}^M$	$g_{\|}$	$g_{\perp}$	$A_{\|}{}^M$	$A_{\perp}{}^M$
[Re(NS)Cl(PPh$_3$)(L^{OMe})]Cl (**4a**Cl)	1.995	420	1.842	1.986	644	330
[Tc(NS)Cl(PPh$_3$)(L^{OMe})]Cl (**4b**Cl)	2.007	168	1.966	2.023	252	112
[Re(NS)Cl$_2$(L^{OMe})] (**5a**)	1.990	455	1.945	1.760	787	398
[Tc(NS)Cl$_2$(L^{OMe})] (**5b**)	1.996	177	1.943	2.021	285	129

Superhyperfine interactions due to couplings of the unpaired electron with the ^{31}P nuclei of the PPh_3 ligands in compounds **4** are not visible. This prevents us from obtaining direct information about the extent of spin delocalization into the ligand orbitals. Indirect information, however, can be deduced from the $^{185,187}Re$ coupling parameters. As described for compounds **1** and **2**, also for the $\{L^{OMe}\}^-$ thionitrosyl complexes, the isotropic and anisotropic A^{Tc} and A^{Re} coupling parameters decrease, when phosphine ligands are present in the equatorial coordination spheres of the metals instead of Cl^-. This can be understood by the transfer of electron density to the π-acceptor PPh_3. The experimental line-widths of the spectra, however, do not allow for the resolution of such couplings for the complexes of the present study.

3. Materials and Methods

$[ReNCl_2(PPh_3)_2]$ [103], $[TcNCl_2(PPh_3)_2]$ [104], $(NBu_4)[TcNCl_4]$ [105], $(NBu_4)[ReNCl_4]$ [106], $[ReNCl(PPh_3)(L^{OMe})]$ [98], $[TcNCl(PPh_3)(L^{OMe})]$ [58], $[ReNCl_2(L^{OMe})]$ [107], $[TcNCl_2(L^{OMe})]$ [58], $[Tc(NS)Cl_3(PPh_3)_2]$ [108] and HEt_2btu [109] were prepared according to literature procedures. All other chemicals were reagent-grade and purchased commercially. Reactions with air- or moisture-sensitive compounds were performed with the standard Schlenk technique. A laboratory approved for the handling of radioactive material was used for the synthesis of the technetium compounds. Normal glassware gives adequate protection against the weak beta radiation of ^{99}Tc as long as small amounts of this isotope as in the present paper are used.

3.1. Syntheses

*[Re(NS)Cl$_3$(PPh$_3$)$_2$] (**1**)*: $[ReNCl_2(PPh_3)_2]$ (2 g, 2.6 mmol) was suspended in 40 mL CH_2Cl_2 and an excess of S_2Cl_2 (0.5 mL, 6.26 mmol) and PPh_3 (680 mg, 5.2 mmol) was added. The mixture was heated under reflux for approximately 30 min, which resulted in a slow dissolution of the starting material and the formation of a dark-red solution. The progress of the reaction can be controlled by TLC. After a complete consumption of $[ReNCl_2(PPh_3)_2]$, the solvent and the remaining S_2Cl_2 were removed in vacuum. The resulting solid was crystallized from a CH_2Cl_2/acetone (1:1) mixture giving dark-red crystals. Yield: 1.49 g (66%). Elemental analysis: Calcd. For $C_{36}H_{30}Cl_3NP_2ReS$: C, 50.1; H, 3.5; N, 1.6; S, 3.7%. Found: C 49.8; H, 3.5; N, 1.6; S, 4.0%. IR (ATR, cm^{-1}): 3057 (w), 1981 (w), 1670 (w), 1586 (w), 1574 (w), 1482 (s), 1434 (s), 1316 (m), 1213 (s), 1187 (s), 1159 (m), 1089 (s), 1074 (m), 1028 (m), 998 (m), 928 (w), 855 (w), 758 (m), 744 (s), 711 (m), 692 (s), 617 (w). EPR (77 K, CH_2Cl_2): $g_x = 2.110$, $g_y = 1.991$, $g_z = 1.943$; $A_x^{Re} = 281 \times 10^{-4}$ cm^{-1}, $A_y^{Re} = 283 \times 10^{-4}$ cm^{-1}, $A_z^{Re} = 524 \times 10^{-4}$ cm^{-1}. EPR (RT, CH_2Cl_2): $g_0 = 2.025$; $a_0^{Re} = 342 \times 10^{-4}$ cm^{-1}. ESI^+ MS (m/z): 885.002 $[M+Na]^+$ (calcd. 885.009), 900.975 $[M+K]^+$ (calcd. 900.983).

*[Re(NS)Cl$_3$(PPh$_3$)(OPPh$_3$)] (**2**)*: The product was obtained as a side product of the synthesis of $[Re(NS)Cl_3(PPh_3)_2]$ when no additional PPh_3 was added. It could be isolated as an orange-red solid following compound **1** during the crystallization procedure. Yield: 0.6 g (26%). IR (ATR, cm^{-1}): 3056 (w), 1589 (w), 1482 (m), 1435 (s), 1231 (s), 1188 (w), 1140 (vs), 1119 (vs), 1026 (m), 998 (m), 924 (w), 852 (w), 747 (s), 723 (vs), 690 (vs). EPR (77 K, acetone): $g_{\|} = 1.923$, $g_{\perp} = 2.008$; $A_{\|}^{Re} = 594 \times 10^{-4}$ cm^{-1}, $A_{\perp}^{Re} = 293 \times 10^{-4}$ cm^{-1}. EPR (RT, acetone): $g_0 = 2.017$; $a_0^{Re} = 372 \times 10^{-4}$ cm^{-1}.

*[Re(NS)(PPh$_3$)(Et$_2$btu)$_2$] (**3a**)*: $[Re(NS)Cl_3(PPh_3)_2]$ (100 mg, 0.1 mmol) was dissolved in 30 mL CH_2Cl_2 and a solution of HEt_2btu (60 mg, 0.25 mmol) in 20 mL Ethanol containing 3 drops of triethylamine was added. The mixture was stirred at room temperature for 30 min. During this time, the color changed to pale brown. The volatiles were removed in vacuum and the remaining solid was subsequently washed with cold methanol, diethyl ether and *n*-hexane. The raw product was dissolved in CH_2Cl_2 for crystallization. Slow evaporation of the solvent gave red-brown crystals. Yield: 31 mg (25%). Elemental analysis: Calcd. for $C_{42}H_{45}N_5O_2PReS_3$: C, 52.3; H, 4.7; N, 7.3; S, 10.0%. Found: C 52.0; H, 4.9; N, 6.8; S, 10.2%. IR (ATR, cm^{-1}): 3058 (w), 2972 (w), 2927 (w), 1599 (w), 1587 (w), 1528 (m), 1499 (s), 1446 (m), 1416 (s), 1394 (s), 1353 (s),1311 (m), 1294 (m),

1251 (s),1210 (w), 1140 (m), 1092 (m), 1071 (m), 1025 (m), 997 (m), 895 (m), 883 (m), 827 (m), 797 (m), 752 (w), 742 (m), 702 (s), 692 (s), 671 (m), 661 (m), 619 (w). ^{1}H NMR (400 MHz, $CDCl_3$, ppm): 8.10 (d, J = 7.6 Hz, 2H, Ph), 7.65 (d, J = 7.3 Hz, 6H, Ph), 7.37–7.13 (m, 15H), 7.01 (t, J = 7.9 Hz, 2H, Ph), 4.37 (dq, J = 14.2, 7.1 Hz, 1H, CH_2), 4.14–3.80 (m, 4H, CH_2), 3.73 (q, J = 7.3, 6.8 Hz, 1H, CH_2), 3.62 (q, J = 6.3 Hz, 1H, CH_2), 3.51 (dd, J = 12.9, 6.5 Hz, 1H, CH_2), 1.52 (s, 2H), 1.39 (dd, J = 9.6, 4.2 Hz, 3H, CH_3), 1.27 (q, J = 12.3, 9.7 Hz, 3H, CH_3), 1.03 (t, J = 6.5 Hz, 3H, CH_3), 0.90 (d, J = 6.3 Hz, 3H, CH_3). J = 8.0 Hz, 12H, CH_3). ^{31}P NMR (CDCl3, ppm): 21.67 (s). ESI$^+$ MS (*m*/*z*): = 965.237 $[M]^+$ (calcd. 965.203) 988.225 $[M+Na]^+$ (calcd. 988.192), 1004.202 $[M+K]^+$ (calcd. 1004.166).

$[Re(NS)Cl(PPh_3)(L^{OMe})]Cl$ (**4a**Cl): $[ReNCl(PPh_3)(L^{OMe})]$ (250 mg, 0.25 mmol) was suspended in 30 mL CH_2Cl_2, an excess of S_2Cl_2 (0.1 mL) was added and the mixture was heated under reflux for 30 min. The solvent was reduced to 15 mL and *n*-hexane (150 mL) was added. The resulting precipitate was washed with hexane and diethyl ether and dried. Recrystallization from a CH_2Cl_2/*n*-hexane (2:1) mixture gave a pale-yellow solid. Yield: 211 mg (83%). Elemental analysis: Calcd. for $C_{29}H_{38}Cl_2CoNO_9P_4ReS$: C, 34.3; H, 3.8; N, 1.4; S, 3.2%. Found: C 34.0; H, 4.0; N, 1.4; S, 3.1%. IR (ATR, cm^{-1}): 3056 (w), 2992 (w), 2948 (w), 1634 (w), 1483 (w), 1457 (w), 1436 (m), 1223 (m), 1177 (m), 1036 (vs), 1014 (vs), 943 (s), 912 (s), 853 (s), 793 (s), 746 (vs), 693 (s), 599 (vs). EPR (77 K, CH_2Cl_2): $g_{\|}$ = 1.842, $g_{\perp}$ = 1.986; $A_{\|}^{Re}$ = 644 × 10^{-4} cm^{-1}, $A_{\perp}^{Re}$ = 330 × 10^{-4} cm^{-1}. EPR (RT, $CHCl_3$): g_0 = 1.995; a_0^{Re} = 420 × 10^{-4} cm^{-1}. ESI$^+$ MS (*m*/*z*): 981.013 $[M]^+$ (calcd. 980.979).

$[Re(NS)Cl(PPh_3)(L^{OMe})](PF_6)$ (***4a**(PF$_6$)*): $[Re(NS)Cl(PPh_3)(L^{OMe})]Cl$ (50 mg, 0.05 mmol) was dissolved in acetonitrile and an excess of $AgPF_6$ (19 mg, 0.075 mmol) was added. The solution was stirred at room temperature and the formed colorless precipitate was removed by filtration. Orange-yellow needles suitable for X-ray diffraction formed upon the slow evaporation of a solution of the complex in CH_2Cl_2/*n*-hexane. Yield: 52 mg (93%). The essential spectroscopic data are identical with those of **4a**Cl.

$[Re(NS)Cl_2(L^{OMe})]$ (***5a***): $[ReNCl_2(L^{OMe})]$ (34 mg, 0.05 mmol) was dissolved in 5 mL CH_2Cl_2 and 3 drops of S_2Cl_2 were added. The mixture was stirred at room temperature. The progress of the reaction can readily be monitored by EPR spectroscopy and typically after 15 min the signals of the starting material have disappeared. The solvent and residual S_2Cl_2 were removed in vacuum and the solid residue was washed subsequently with *n*-hexane and diethyl ether. The product was recrystallized from CH_2Cl_2/diethyl ether giving a pale-brown, microcrystalline solid. Yield: 20 mg (53%). IR (ATR, cm^{-1}): 3111 (w), 2958 (m), 2874 (w), 1460 (w), 1425 (w), 1381 (w), 1260 (w), 1222 (s), 1175 (s), 1012 (vs), 945 (w), 860 (m), 796 (vs), 743 (s), 595 (m). EPR (77 K, CH_2Cl_2): $g_{\|}$ = 1.945, $g_{\perp}$ = 1.760; $A_{\|}^{Re}$ = 787 × 10^{-4} cm^{-1}, $A_{\perp}^{Re}$ = 398 × 10^{-4} cm^{-1}. EPR (RT, $CHCl_3$): g_0 = 1.990; a_0^{Re} = 455 × 10^{-4} cm^{-1}. ESI$^+$ MS (*m*/*z*): 776.846 $[M+Na]^+$ (ber.: 776.847); 792.821 $[M+K]^+$ (ber.: 792.821).

$[Tc(NS)Cl(PPh_3)(L^{OMe})]Cl$ (**4b**Cl): $[TcNCl(PPh_3)(L^{OMe})]$ (72 mg, 0.08 mmol) was dissolved in 2 mL CH_2Cl_2 (2 mL) and S_2Cl_2 (11 mg, 0.08 mmol) was added under permanent stirring. The stirring was continued at room temperature for 1 h and the obtained dark-red mixture was filtered to remove some insoluble solid (most probably elemental sulfur). All volatiles were removed in vacuum and the remaining solid crystallized from a CH_2Cl_2/*n*-pentane (1:1) mixture. Storing such a mixture in a refrigerator for several days gave a red, microcrystalline powder. Yield: 11 mg (15%). IR (KBr, cm^{-1}): 2910 (vs), 2723 (s), 1726 (m), 1630 (w) 1479 (vs), 1381 (vs), 1227 (vs), 1171 (m), 1040 (w), 949 (s), 928 (s), 851 (w), 802 (w), 723 (m), 610 (w), 542 (m). EPR (77 K, CH_2Cl_2): $g_{\|}$ = 1.966, $g_{\perp}$ = 2.023; $A_{\|}^{Tc}$ = 252 × 10^{-4} cm^{-1}, $A_{\perp}^{Tc}$ = 112 × 10^{-4} cm^{-1}. EPR (RT, CH_2Cl_2): g_0 = 2.007; a_0^{Tc} = 168 × 10^{-4} cm^{-1}.

$[Tc(NS)Cl_2(L^{OMe})]$ (***5b***): $[TcNCl_2(L^{OMe})]$ (41 mg, 0.06 mmol) was dissolved in CH_2Cl_2 (10 mL) and treated with an excess of S_2Cl_2 (0.3 mL). After stirring for 30 min at room temperature, all volatiles were removed in vacuum. The remaining solid was washed with *n*-hexane and diethyl ether and dissolved in 1 mL CH_2Cl_2. Overlayering with *n*-hexane and storing in a refrigerator for several days gave pale-red crystals. Yield: 32 mg (75%). IR (KBr, cm^{-1}): 3107 (w), 3086 (w), 2990 (w), 2841 (w), 1462 (w), 1423 (w), 1310 (vs), 1236 (vs),

1182 (vs), 1128 (vs), 1098 (vs), 986 (vs), 847 (m), 795 (s), 747 (s), 638 (m), 608 (s), 530 (w), 476 (w), 426 (w). EPR (77 K, CH_2Cl_2): $g_{\|}$ = 1.943, $g_{\perp}$ = 2.021, $A_{\|}^{Tc}$ = 285 × 10^{-4} cm^{-1}, $A_{\perp}^{Tc}$ = 129 × 10^{-4} cm^{-1}. EPR (RT, CH_2Cl_2) g_0 = 1.996; a_0^{Tc} = 177 × 10^{-4} cm^{-1}.

3.2. Spectroscopic and Analytical Methods

Elemental analyses of carbon, hydrogen, nitrogen and sulfur were determined using a Heraeus vario EL elemental analyzer. IR spectra were measured as KBr pellets on a Shimadzu IR Affinity-1 (technetium compounds) or a Thermo Scientific Nicolet iS10 ATR spectrometer (rhenium complexes). The NMR spectra were recorded on JEOL ECS-400 or ECZ-400 400 MHz spectrometers. ESI TOF mass spectra were measured with an Agilent 6210 ESI TOF (Agilent Technologies, Santa Clara, CA, USA). X-Band EPR spectra were recorded in solution with a Magnettech Miniscope MS400 spectrometer at 300 and 77 K. Simulation and visualization of the EPR spectra were conducted with the EasySpin tool box in MatLab [110,111].

3.3. X-ray Crystallography

The intensities for the X-ray determinations were collected on STOE IPDS-2T or Bruker CCD instruments with Mo/Kα radiation. The various temperatures applied are due to the experimental setup of the different diffractometers. Semi-empirical or numerical absorption corrections were carried out by the SADABS or X-RED32 programs [112,113]. Structure solution and refinement were performed with the SHELX programs [114,115] included in the WinGX [116] program package or OLEX2 [117]. Hydrogen atoms were calculated for idealized positions and treated with the "riding model" option of SHELXL. The solvent mask option of OLEX2 was applied to treat diffuse electron density due to disordered CH_2Cl_2 in the crystals of [Re(NS)Cl_3(PPh_3)($OPPh_3$)] (**2**). Details are given in the Supplementary Materials. The representation of molecular structures was conducted using the program DIAMOND [118].

4. Conclusions

Reactions of rhenium and technetium nitrido compounds with disulfur dichloride give access to novel thionitrosyl complexes of these elements having monodentate and chelating ligands in their coordination spheres. The new compounds are chemically related to corresponding nitrosyl complexes but do not possess their robustness and stability. Their thermal instability and the lack of a suitable one-step synthesis starting from pertechnetate set narrow limits for potential applications in nuclear medical procedures, as is discussed in the introduction.

Supplementary Materials: The following supporting information can be downloaded at https://www.mdpi.com/article/10.3390/inorganics12080210/s1, Table S1.1: Crystallographic data and data collection parameters; Figure S1.1: Ellipsoid representation of [Re(NS)Cl_3(PPh_3)$_2$] (**1**). The thermal ellipsoids are set at a 50% probability level. Hydrogen atoms are omitted for clarity; Table S1.2: Selected bond lengths (Å) and angles (°) in the [Re(NS)Cl_3(PPh_3)$_2$] (**1**); Figure S1.2: Ellipsoid representation of two crystallographically independent molecules of [Re(NS)Cl_3(PPh_3)($OPPh_3$)] (**2**). The thermal ellipsoids are set at a 50% probability level. Hydrogen atoms are omitted for clarity; Table S1.3.: Selected bond lengths (Å) and angles (°) in [Re(NS)Cl_3(PPh_3)($OPPh_3$)] (**2**); Figure S1.5: Ellipsoid representation of [Re(NS)(PPh_3)(Et_2btu)$_2$] (**3a**). The thermal ellipsoids are set at a 35% probability level. Hydrogen atoms are omitted for clarity; Table S1.6: Selected bond lengths (Å) and angles (°) in [Re(NS)(PPh_3)(Et_2btu)$_2$] (**3a**); Figure S1.3: Ellipsoid representation of [Re(NS)Cl(PPh_3)(L^{OMe})] (PF_6) (**4a**(PF_6)) including the positional disorder between the Re–N–S and Re–Cl bonds. The thermal ellipsoids are set at a 50% probability level. Hydrogen atoms are omitted for clarity; Table S1.4: Selected bond lengths (Å) and angles (°) in the [Re(NS)Cl(PPh_3)(L^{OMe})]$^+$ (**4a**) cation; Figure S1.4: Ellipsoid representation of two crystallographically independent molecules of [Tc(NS)Cl_2(L^{OMe})] (**5b**) including the positional disorder for the O atoms of the {L^{OMe}}$^-$ ligands and between the Tc–N–S and the Tc–Cl bonds. The thermal ellipsoids are set at a 50% probability level; Table S1.5: Selected bond lengths (Å) and angles (°) in [Tc(NS)Cl_2(L^{OMe})] (**5b**); Figure S2.1: IR

(ATR) spectrum of [Re(NS)Cl_3(PPh_3)$_2$] (**1**); Figure S2.2: Solution EPR spectra of [Re(NS)Cl_3(PPh_3)$_2$] (**1**) in CH_2Cl_2, (a) at room temperature and (b) at T = 77 K; Figure S2.3: ESI(+) mass spectrum of [Re(NS)Cl_3(PPh_3)$_2$] (**1**) in CH_3CN; Figure S2.4: IR spectrum (ATR) of [Re(NS)Cl_3(PPh_3)($OPPh_3$)] (**2**); Figure S2.5: Solution EPR spectra of [Re(NS)Cl_3(PPh_3)($OPPh_3$)] (**2**) in acetone; (a) at room temperature and (b) at T = 77 K; Figure S2.6: ESI(+) mass spectrum of [Re(NS)Cl_3(PPh_3)($OPPh_3$)] (**2**) in CH_3CN; Figure S2.7: IR spectrum (ATR) of [Re(NS)(PPh_3)(Et_2btu)$_2$] (**3a**); Figure S2.8: ^{1}H NMR spectrum of [Re(NS)(PPh_3)(Et_2btu)$_2$] (**3a**) in $CDCl_3$; Figure S2.9: ^{31}P NMR spectrum of [Re(NS)(PPh_3)(Et_2btu)$_2$] (**3a**) in $CDCl_3$; Figure S2.10: ESI(+) mass spectrum [Re(NS)(PPh_3)(Et_2btu)$_2$] (**3a**) in CH_3CN; Figure S2.11: IR spectrum (ATR) of [Re(NS)Cl(PPh_3)(L^{OMe})]Cl (**4a**Cl); Figure S2.12: Solution EPR spectra of [Re(NS)Cl(PPh_3)(L^{OMe})]Cl (**4a**Cl) in CH_2Cl_2; (a) at room temperature and (b) at T = 77 K; Figure S2.13: ESI(+) mass spectrum of [Re(NS)Cl(PPh_3)(L^{OMe})]Cl (**4a**Cl) in CH_3CN; Figure S2.14: IR spectrum (ATR) of [Re(NS)Cl(PPh_3)(L^{OMe})](PF_6) (**4a**(PF_6)); Figure S2.15: ESI(+) mass spectrum of [Re(NS)Cl(PPh_3)(L^{OMe})](PF_6) (**4a**(PF_6)) in CH_3CN; Figure S2.16: IR spectrum (ATR) of [Re(NS)Cl_2(L^{OMe})] (**5a**); Figure S2.17: Solution EPR spectra of [Re(NS)Cl_2(L^{OMe})] (**5a**) in CH_2Cl_2; (a) at room temperature and (b) at T = 77 K; Figure S2.18: ESI(+) mass spectrum of [Re(NS)Cl(PPh_3)(L^{OMe})](PF_6) (**4a**(PF_6)) in CH_3CN; Figure S2.19: IR spectrum (KBr) of [Tc(NS)Cl(PPh_3)(L^{OMe})]Cl (**4b**Cl); Figure S2.20: Solution EPR spectra of [Tc(NS)Cl(PPh_3)(L^{OMe})]Cl (**4b**Cl) in CH_2Cl_2; (a) at room temperature and (b) at T = 77 K; Figure S2.21: IR spectrum (KBr) of [Tc(NS)Cl_2(L^{OMe})] (**5b**); Figure S2.22: Solution EPR spectra of [Tc(NS)Cl_2(L^{OMe})] (**5b**). in CH_2Cl_2; (a) at room temperature and (b) at T = 77 K.

Author Contributions: Conceptualization, U.A. and D.N.; methodology, D.N. and A.H.; validation, A.H., T.E.S. and D.N.; formal analysis, D.N. and T.E.S.; investigation, D.N.; resources, U.A.; data curation, D.N. and A.H.; writing—original draft preparation, U.A.; writing—review and editing, D.N.; A.H. and T.E.S.; visualization, D.N. and U.A.; supervision, U.A.; project administration, U.A.; funding acquisition, U.A. All authors have read and agreed to the published version of the manuscript.

Funding: This research was funded by Freie Universität Berlin and the Deutsche Forschungsgemeinschaft (Core Facility BIOSUPRAMOL).

Data Availability Statement: Additional data are contained within the article and Supplementary Materials.

Acknowledgments: We would like to acknowledge the assistance of the Core Facility BioSupraMol supported by the DFG.

Conflicts of Interest: The authors declare no conflicts of interest.

References

1. *Technetium-99m Radiopharmaceuticals: Manufacture of Kits*; IAEA Technical Reports Series No. 466; International Atomic Energy Agency: Vienna, Austria, 2008; pp. 126–129.
2. Abram, U.; Alberto, R. Technetium and rhenium—coordination chemistry and nuclear medical applications. *J. Braz. Chem. Soc.* **2006**, *17*, 1486–1500. [CrossRef]
3. Bartholomä, M.D.; Louie, A.S.; Valliant, J.F.; Zubieta, J. Technetium and gallium derived radiopharmaceuticals: Comparing and contrasting the chemistry of two important radiometals for the molecular imaging era. *Chem. Rev.* **2010**, *110*, 2903–2920. [CrossRef] [PubMed]
4. Bhattacharyya, S.; Dixit, M. Metallic radionuclides in the development of diagnostic and therapeutic radiopharmaceuticals. *Dalton Trans.* **2011**, *40*, 6112–6128. [CrossRef] [PubMed]
5. Liu, S.; Chakraborty, S. ^{99m}Tc-centered one-pot synthesis for preparation of ^{99m}Tc radiotracers. *Dalton Trans.* **2011**, *40*, 6077–6086. [CrossRef] [PubMed]
6. Dilworth, J.R.; Pascu, S.I. The Radiopharmaceutical Chemistry of Technetium and Rhenium. In *The Chemistry of Molecular Imaging*; Long, N., Wong, W.-T., Eds.; John Wiley & Sons: Chichester, UK, 2015; pp. 163–174.
7. Kuntic, V.; Brboric, J.; Vujic, Z.; Uskokovic-Markovic, S. Radioisotopes Used as Radiotracers in vitro and in vivo Diagnostics: A Review. *Asian J. Chem.* **2016**, *28*, 235–411. [CrossRef]
8. Papagiannopoulou, D. Technetium-99m radiochemistry for pharmaceutical applications. *J. Labelled Compd. Radiopharm.* **2017**, *60*, 502–520. [CrossRef] [PubMed]
9. Duatti, A. Review on ^{99m}Tc radiopharmaceuticals with emphasis on new advancements. *Nucl. Med. Biol.* **2021**, *92*, 202–216. [CrossRef] [PubMed]
10. Alberto, R.; Nadeem, Q. ^{99m}Technetium-Based Imaging Agents and Developments in ^{99}Tc Chemistry. In *Metal Ions in Bio-Imaging Techniques*; Sigel, A., Freisinger, E., Sigel, K.O., Eds.; De Gruyter: Berlin/Munich, Germany; Boston, MA, USA, 2021; pp. 196–238.

11. Alberto, R. Role of Pure Technetium Chemistry: Are There Still Links to Applications in Imaging? *Inorg. Chem.* **2023**, *62*, 20539–20548. [CrossRef] [PubMed]
12. World Nuclear Association. Radioisotopes in Medicine. Available online: https://world-nuclear.org/information-library/non-power-nuclear-applications/radioisotopes-research/radioisotopes-in-medicine (accessed on 1 July 2024).
13. Dash, A.; Knapp, F.F., Jr.; Pillai, M.R.A. ^{99}Mo/^{99m}Tc separation: An assessment of technology options. *Nucl. Med. Biol.* **2013**, *40*, 167–176. [CrossRef]
14. Lepareur, N.; Lacœuille, F.; Bouvry, C.; Hindré, F.; Garcion, E.; Chérel, M.; Noiret, N.; Garin, E.; Knapp, F.F. Rhenium-188 Labeled Radiopharmaceuticals: Current Clinical Applications in Oncology and Promising Perspectives. *Front. Med.* **2019**, *6*, 132. [CrossRef]
15. Cutler, C.S.; Hennkens, H.M.; Sisay, N.; Huclier-Markai, S.; Jurisson, S. Radiometals for Combined Imaging and Therapy. *Chem. Rev.* **2013**, *113*, 858–883. [CrossRef]
16. Price, E.W.; Orvig, C. Matching chelators to radiometals for radiopharmaceuticals. *Chem. Soc. Rev.* **2014**, *43*, 260–290. [CrossRef]
17. Kronauge, J.F.K.; Mindiola, D.J. The value of Stable Metal-Carbon Bonds in Nuclear Medicine and the Cardiolite Story. *Organometallics* **2016**, *35*, 3432–3435. [CrossRef]
18. Morais, G.R.; Paulo, A.; Santos, I. Organometallic Complexes for SPECT Imaging and/or Radionuclide Therapy. *Organometallics* **2012**, *31*, 5693–5714. [CrossRef]
19. Alberto, R. From oxo to carbonyl and arene complexes; A journey through technetium chemistry. *J. Organomet. Chem.* **2018**, *869*, 264–269. [CrossRef]
20. Benz, M.; Braband, H.; Schmutz, P.; Halter, J.; Alberto, R. From Tc^{VII} to Tc^{I}; facile syntheses of bis-arene complexes $[^{99(m)}Tc(arene)_2]^+$ from pertechnetate. *Chem. Sci.* **2015**, *6*, 165–169. [CrossRef]
21. Meola, G.; Braband, H.; Jordi, S.; Fox, T.; Blacque, O.; Spingler, B.; Alberto, R. Structure and reactivities of rhenium and technetium bis-arene sandwich complexes $[M(\eta^6\text{-arene})_2]^+$. *Dalton Trans.* **2017**, *46*, 14631–14637. [CrossRef]
22. Nadeem, Q.; Meola, G.; Braband, H.; Bollinger, R.; Blancque, O.; Hernandez-Valdes, D.; Alberto, R. To Sandwich Technetium: Highly Functionalized Bis-Arene Complexes $[^{99m}Tc(\eta^6\text{-arene})_2]^+$ Directly from Water and $[TcO_4^-]$. *Angew. Chem. Int. Ed. Engl.* **2020**, *59*, 1197–1200. [CrossRef] [PubMed]
23. Nadeem, Q.; Battistin, F.; Blancque, O.; Alberto, R. Naphtalene Exchange in $[Re(\eta^6\text{-napht})_2]^+$ with Pharmaceutical Leads to Highly Functionalized Sandwich Complexes $[M(\eta^6\text{-pharm})_2]^+$ (M = Re/^{99m}Tc). *Chemistry* **2022**, *28*, e202103566. [CrossRef]
24. Boschi, A.; Uccelli, L.; Marvelli, L.; Cittanti, C.; Giganti, M.; Martini, P. Technetium-99m Radiopharmaceuticals for Ideal Myocardial Perfusion Imaging: Lost and Found Opportunities. *Molecules* **2022**, *27*, 1188. [CrossRef]
25. Pasqualini, R.; Duatti, A.; Bellande, E.; Comazzi, V.; Brucato, V.; Hoffschir, D.; Fagret, D.; Comet, M. Bis (Dithiocarbamato) Nitrido Technetium-99m Radiopharmaceuticals: A Class of Neutral Myocardial Imaging Agents. *J. Nucl. Med.* **1994**, *35*, 334–341.
26. Boschi, A.; Uccelli, L.; Bolzati, C.; Duatti, A.; Sabba, N.; Moretti, E.; di Domenico, G.; Zavattini, G.; Refosco, F.; Giganti, M. Synthesis and Biologic Evaluation of Monocationic Asymmetric ^{99m}Tc-Nitride Heterocomplexes Showing High Heart Uptake and Improved Imaging Properties. *J. Nucl. Med.* **2003**, *44*, 806–814. [PubMed]
27. Salvarese, N.; Carta, D.; Marzano, C.; Gerardi, G.; Melendez-Alafort, L.; Bolzati, C. $[^{99m}Tc][Tc(N)(DASD)(PNPn)]^+$ (DASD = 1,4-Dioxa-8-Azaspiro[4,5]Decandithiocarbamate, PNP n = Bisphosphinoamine) for Myocardial Imaging: Synthesis, Pharmacological and Pharmacokinetic Studies. *J. Med. Chem.* **2018**, *61*, 11114–11126. [CrossRef] [PubMed]
28. Meszaros, L.K.; Dose, A.; Biagini, S.C.G.; Blower, P.J. Hydrazinonicotinic acid (HYNIC)—Coordination chemistry and applications in radiopharmaceutical chemistry. *Inorg. Chim. Acta* **2010**, *363*, 1059–1069. [CrossRef]
29. Abrams, M.J.; Juweid, M.; tenKate, C.I.; Schwartz, D.A.; Hauser, M.M.; Gaul, F.E.; Fuccello, A.J.; Rubin, R.H.; Strauss, H.W.; Fischman, A.J. Technetium-99m-human polyclonal IgG radiolabeled via the hydrazine nicotinamide derivative for imaging focal sites of infection in rats. *J. Nucl. Med.* **1990**, *31*, 2022–2028. [PubMed]
30. Jiang, Y.; Tian, Y.; Feng, B.; Zhao, T.; Yu, X.; Zhao, Q. A novel molecular imaging probe $[^{99m}Tc]$Tc-HYNIC-FAPI targeting cancer-associated fibroblasts. *Sci. Rep.* **2023**, *13*, 3700. [CrossRef] [PubMed]
31. Cheah, C.T.; Newman, J.L.; Nowotnik, D.P.; Thornback, J.R. Synthesis and biological studies of the $[^{99m}Tc]$tetrachloronitrosyltechnetium(II) anion—An alternative low valent technetium starting material. *Int. J. Rad. Appl. Instrum. Nucl. Med. Biol.* **1987**, *14*, 573–575. [CrossRef] [PubMed]
32. Machura, B. Structural and spectroscopic properties of rhenium nitrosyl complexes. *Coord. Chem. Rev.* **2005**, *249*, 2277–2307. [CrossRef]
33. Dilworth, J.R. Rhenium chemistry—Then and Now. *Coord. Chem. Rev.* **2021**, *436*, 213822. [CrossRef]
34. Mahmood, A.; Akgun, Z.; Peng, Y.; Mueller, P.; Jiang, Y.; Berke, H.; Jones, A.G.; Nicholson, T. The synthesis and characterization of rhenium nitrosyl complexes. The X-ray crystal structures of $[ReBr_2(NO)(NCMe)_3]$, $[Re(NO)(N_5)](BPh_4)_2]$ and $[ReBr_2(NO)(NCMe)\{py\text{-}CH2\text{-}NHCH_2CH_2\text{-}N(CH_2\text{-}py)_2\}]$. *Inorg. Chim. Acta* **2013**, *405*, 455–460. [CrossRef]
35. Abram, U.; Ortner, K.; Hübener, R.; Voigt, A.; Caballho, R.; Vazquez-Lopez, E. Darstellung, Strukturen und EPR-Spektren der Rhenium(II)-Nitrosylkomplexe $[Re(NO)Cl_2(PPh_3)(OPPh_3)(OReO_3)]$, $[Re(NO)Cl_2(OPPh_3)_2(OReO_3)]$ und $[Re(NO)Cl_2(PPh_3)_3][ReO_4]$. *Z. Anorg. Allg. Chem.* **1998**, *624*, 1662–1668. [CrossRef]
36. Agbossou, F.; O'Connor, E.J.; Garner, C.M.; Quiros Mendez, N.; Fernandez, J.M.; Patton, A.T.; Ramsden, J.A.; Gladysz, J.A. Cyclopentadienyl Rhenium Complexes. *Inorg. Synth.* **1992**, *29*, 211–225.

37. Seidel, S.N.; Prommesberger, M.; Eichenseher, S.; Meyer, O.; Hampel, F.; Gladysz, J.A. Syntheses and structural analyses of chiral rhenium containing amines of the formula (η^5-C_5H_5)Re(NO)(PPh_3)((CH_2)$_n$NRR′) (n = 0, 1). *Inorg. Chim. Acta* **2010**, *363*, 533–548. [CrossRef]
38. Bernasconi, C.F.; Bhattacharya, S.; Wenzel, P.J.; Olmstead, M.M. Kinetic and Thermodynamic Acidity of [Cp(NO)(PPh_3)Re(2,5-dimethyl-3-thienyl)carbene]$^+$. Transition State Imbalance and Intrinsic Barriers. *Organometallics* **2006**, *25*, 4322–4330. [CrossRef]
39. Dilsky, S.; Schenk, W.A. Diastereomeric Halfsandwich Rhenium Complexes Containing Hemilabile Phosphane Ligands. *Eur. J. Inorg. Chem.* **2004**, *2004*, 4859–4870. [CrossRef]
40. Nicholson, T.; Chun, E.; Mahmood, A.; Mueller, P.; Davison, A.; Jones, A.G. Synthesis, spectroscopy and structural analysis of Technetium and Rhenium nitrosyl complexes. *Commun. Inorg. Chem.* **2015**, *3*, 31–39.
41. Blanchard, S.S.; Nicholson, T.; Davison, A.; Davis, W.; Jones, A.G. The synthesis, characterization and substitution reactions of the mixed technetium(I) nitrosyl complex *trans-trans*-[(NO)($NCCH_3$)Cl_2(PPh_3)$_2$Tc]. *Inorg. Chim. Acta* **1996**, *244*, 121–130. [CrossRef]
42. Balasekaran, S.M.; Hagenbach, A.; Drees, M.; Abram, U. [Tc^{II}(NO)(trifluoroacetate)$_4$F]$^{2-}$—Synthesis and reactions. *Dalton Trans.* **2017**, *46*, 13544–13552. [CrossRef] [PubMed]
43. Linder, K.E.; Davison, A.; Dewan, J.C.; Costello, C.E.; Melaknia, S. Nitrosyl complexes of technetium: Synthesis and characterization of [Tc^{I}(NO)($CNCMe_3$)$_5$](PF_6)$_2$ and Tc(NO)Br_2($CNCMe_3$)$_3$ and the crystal structure of Tc(NO)Br_2($CNCMe_3$)$_3$. *Inorg. Chem.* **1986**, *25*, 2085–2089. [CrossRef]
44. Ackermann, J.; Noufele, C.N.; Hagenbach, A.; Abram, U. Nitrosyltechnetium(I) Complexes with 2-(Diphenylphosphanyl)aniline. *Z. Anorg. Allg. Chem.* **2019**, *645*, 8–13. [CrossRef]
45. Ackermann, J.; Hagenbach, A.; Abram, U. {Tc(NO)(Cp)(PPh_3)}$^+$—A novel technetium(I) core. *Chem. Commun.* **2016**, *52*, 10285–10288. [CrossRef]
46. Ackermann, J.; Abdulkader, A.; Scholtysik, C.; Jungfer, M.R.; Hagenbach, A.; Abram, U. [Tc^{I}(NO)X(Cp)(PPh_3)] Complexes (X^- = I^-, I_3^-, SCN^-, $CF_3SO_3^-$, or CF_3COO^-) and Their Reactions. *Organometallics* **2019**, *38*, 4471–4478. [CrossRef]
47. Abdulkader, A.; Hagenbach, A.; Abram, U. [Tc(NO)Cl(Cp)(PPh_3)]—A Technetium(I) Compound with an Unexpected Synthetic Potential. *Eur. J. Inorg. Chem.* **2021**, *2021*, 3812–3818.
48. Schibli, R.; Marti, N.; Maurer, P.; Spingler, B.; Lehaire, M.-L.; Gramlich, V.; Barnes, C.L. Syntheses and Characterization of Dicarbonyl–Nitrosyl Complexes of Technetium(I) and Rhenium(I) in Aqueous Media: Spectroscopic, Structural, and DFT Analyses. *Inorg. Chem.* **2005**, *44*, 683–690. [CrossRef]
49. Brown, D.S.; Newman, J.L.; Thornback, J.R.; Davison, A. Structure of the tetra-*n*-butylammoium salt of tetrachloro(methanol) nitrosyltechnetium(II) anion. *Acta Cryst.* **1987**, *C43*, 1692–1694.
50. Brown, D.S.; Newman, J.L.; Thornback, J.R.; Pearlstein, R.M.; Davison, A.; Lawson, A. The synthesis and characterisation of the trichloronitrosyl(acetylacetonato)technetium(II) anion, a novel technetium(II) complex. *Inorg. Chim. Acta* **1988**, *150*, 193–196. [CrossRef]
51. Nicholson, T.; Hirsch-Kuchma, M.; Freiberg, E.; Davison, A.; Jones, A.G. The reaction chemistry of a technetium(I) nitrosyl complex with potentially chelating organohydrazines: The X-ray crystal structure of [$TcCl_2$(NO)($HNNC_5H_4N$)(PPh_3)]. *Inorg. Chim. Acta* **1998**, *279*, 206–209.
52. De Vries, N.; Cook, J.; Davison, A.; Nicholson, T.; Jones, A.G. Synthesis and characterization of a technetium(III) nitrosyl compound: Tc(NO)(Cl)($SC_{10}H_{13}$)$_3$. *Inorg. Chem.* **1990**, *29*, 1062–1064. [CrossRef]
53. Nicholson, T.; Mahmood, A.; Limpa-Amara, N.; Salvarese, N.; Takase, M.K.; Müller, P.; Akgun, Z.; Jones, A.G. Reactions of the tridentate and tetradentate amine ligands di-(2-picolyl)(*N*-ethyl)amine and 2,5-bis-(2-pyridylmethyl)-2,5 diazohexane with technetium nitrosyl complexes. *Inorg. Chim. Acta* **2011**, *373*, 301–305. [CrossRef]
54. Roca Jungfer, M.; Ernst, M.J.; Hagenbach, A.; Abram, U. [{Tc^{I}(NO)(L^{OMe})(PPh_3)Cl}$_2$Ag](PF_6) and [Tc^{II}(NO)(L^{OMe})(PPh_3)Cl](PF_6): Two Unusual Technetium Complexes with a "Kläui-type" Ligand. *Z. Anorg. Allg. Chem.* **2022**, *648*, e202100316.
55. Nicholson, T.L.; Mahmood, A.; Muller, P.; Davison, A.; Storm-Blanchard, S.; Jones, A.G. The synthesis and structural characterization of the technetium nitrosyl complexes [TcCl(NO)(SC_5H_4N)(PPh_3)$_2$] and [Tc(NO)(SC_5H_4N)$_2$(PPh_3)]. *Inorg. Chim. Acta* **2011**, *365*, 484–486. [CrossRef] [PubMed]
56. Balasekaran, S.M.; Spandl, J.; Hagenbach, A.; Köhler, K.; Drees, M.; Abram, U. Fluoridonitrosyl Complexes of Technetium(I) and Technetium(II). Synthesis, Characterization, Reactions, and DFT Calculations. *Inorg. Chem.* **2014**, *53*, 5117–5128. [CrossRef]
57. Nicholson, T.; Hirsch-Kuchma, M.; Shellenbarger-Jones, A.; Davison, A.; Jones, A.G. The synthesis and characterization of a technetium nitrosyl complex with cis-{2-pyridyl,diphenylphosphine} coligands. The X-ray crystal structure of [$TcCl_2$(NO)(pyPPh_2-*P*,*N*) (pyPPh_2-*P*)]. *Inorg. Chim. Acta* **1998**, *267*, 319–322. [CrossRef]
58. Grunwald, A.C.; Scholtysik, C.; Hagenbach, A.; Abram, U. One Ligand, One Metal, Seven Oxidation States: Stable Technetium Complexes with the "Kläui Ligand". *Inorg. Chem.* **2020**, *59*, 9396–9405. [CrossRef] [PubMed]
59. Nicholson, T.L.; Mahmood, A.; Refosco, F.; Tisato, F.; Müller, P.; Jones, A.G. The synthesis and X-ray structural characterization of *mer* and *fac* isomers of the technetium(I) nitrosyl complex [$TcCl_2$(NO)(PNPpr)]. *Inorg. Chim. Acta* **2009**, *362*, 3637–3640. [CrossRef] [PubMed]
60. Nicholson, T.; Müller, P.; Davison, A.; Jones, A.G. The synthesis and characterization of a cationic technetium nitrosyl complex: The X-ray crystal structure of [TcCl(NO)(DPPE)$_2$](PF_6) × CH_2Cl_2. *Inorg. Chim. Acta* **2006**, *359*, 1296–1298. [CrossRef]
61. Pandey, K.K. Coordination Chemistry of Thionitrosyl (NS), Thiazate (NSO^-), Disulfidothionitrate (S,N^-), Sulfur Monoxide (SO), and Disulfur Monoxide (S,O) Ligands. *Progr. Inorg. Chem.* **1992**, *40*, 445–502.

62. Døsing, A. The electronic structure and photochemistry of transition metal thionitrosyl complexes. *Coord. Chem. Rev.* **2016**, *306*, 544–557. [CrossRef]
63. Anhaus, J.; Siddiqi, Z.A.; Roesky, H.W. Reaction of Tetrasulfurtetranitride with Rhenium(VII)-chloronitride. The Crystal Structure of $[Ph_4As^+]_2[Cl_4Re(NS)(NSCl)^{2-}] \times CH_2Cl_2$. *Z. Naturforsch.* **1985**, *40b*, 740–744. [CrossRef]
64. Dirican, D.; Pfister, N.; Wozniak, M.; Braun, T. Reactivity of Binary and Ternary Sulfur Halides towards Transition-Metal Compounds. *Chem. Eur. J.* **2020**, *31*, 6945–6963. [CrossRef]
65. Dietrich, A.; Neumüller, B.; Dehnicke, K. $(PPh_4)_2[(SN)ReCl_3(\mu\text{-}N)(\mu\text{-}NSN)ReCl_3(THF)]$—Ein Nitrido-Thionitrosyl-Dinitridosulfato-Komplex des Rheniums. *Z. Anorg. Allg. Chem.* **2000**, *626*, 1268–1270. [CrossRef]
66. Reinel, M.; Höcher, T.; Abram, U.; Kirmse, R. Ein Beitrag zu Rhenium(II)-, Osmium(II)- und Technetium(II)-Thionitrosylkomplexe vom Typ $[M(NS)Cl_4py]$: Darstellung, Strukturen und EPR-Spektren. *Z. Anorg. Allg. Chem.* **2003**, *629*, 853–861. [CrossRef]
67. Voigt, A.; Abram, U.; Kirmse, R. Darstellung, Strukturen und EPR-Spektren der Rhenium(II)-Thionitrosylkomplexe *trans*-$[Re(NS)Cl_3(MePh_2P)_2]$ und *trans*-$[Re(NS)Br_3(Me_2PhP)_2]$. *Z. Anorg. Allg. Chem.* **1999**, *625*, 1658–1663. [CrossRef]
68. Hauck, H.-G.; Willing, W.; Müller, U.; Dehnicke, K. $[ReCl_2(NS)(NSCl)(Pyridin)_2]$, ein Thionitrosyl-chlorthionitrenkomplex des Rheniums. *Z. Anorg. Allg. Chem.* **1986**, *534*, 77–84. [CrossRef]
69. Hübener, R.; Abram, U.; Strähle, J. Isothiocyanato complexes of rhenium II. Synthesis, characterization and structures of $ReN(NCS)_2(Me_2PhP)_3$ and $Re(NS)(NCS)_2(Me_2PhP)_3$. *Inorg. Chim. Acta* **1994**, *216*, 223–228. [CrossRef]
70. Ritter, S.; Abram, U. Gemischtligand-Komplexe des Rheniums. VI. Darstellung und Strukturen der Rhenium Thionitrosyl-Komplexe *mer*-$[Re(NS)Cl_2(Me_2PhP)_3] \times CH_2Cl_2$ und *trans*-$[Re(NS)Cl_3(Me_2PhP)_2]$. *Z. Anorg. Allg. Chem.* **1994**, *620*, 1223–1228.
71. Ritter, S.; Abram, U. Gemischtligandkomplexe des Rheniums. IX. Reaktionen am Nitridoliganden von $[ReN(Me_2PhP)(Et_2dtc)_2]$. Synthese, Charakterisierung und Kristallstrukturen von $[Re(NBCl_3)(Me_2PhP)(Et_2dtc)_2]$, $[Re(NGaCl_3)(Me_2PhP)(Et_2dtc)_2]$ und $[Re(NS)Cl(Me_2PhP)_2(Et_2dtc)]$. *Z. Anorg. Allg. Chem.* **1995**, *622*, 965–973. [CrossRef]
72. Ruf, C.; Behrens, U.; Lork, E.; Mews, R. Reactions of halides with *trans*-$[Re(CO)_4(MeCN)(NS)][AsF_6]_2$: Syntheses and structure of *trans*-$[Re(CO)_4(Cl)(NS)][AsF_6]$ and $[(OC)_5ReNS\text{–}NS\text{–}N[Re(CO)_5]_5\{N\text{–}SNRe(CO)_5\}\text{–}CH_2\text{–}CH_2][AsF_6]_2$, an unusual trinuclear bis(thiazyl)rhenium complex. *Chem. Commun.* **1996**, 939–940. [CrossRef]
73. Baldas, J.; Bonnyman, J.; Mackay, M.F.; Williams, G.A. Structural studies of technetium complexes. V. The preparation and crystal structure of Dichlorobis(diethyldithiocarbamato)thionitrosyltechnetium(III). *Austr. J. Chem.* **1984**, *37*, 751–759. [CrossRef]
74. Kaden, L.; Lorenz, B.; Kirmse, R.; Stach, J.; Behm, H.; Beurskens, P.T.; Abram, U. Synthesis, characterization and x-ray molecular and crystal structure of $Tc(NS)Cl_3(Me_2PhP)(Me_2PhPO)$-a first example of mixed phosphine/phosphine oxide coordination. *Inorg. Chim. Acta* **1990**, *169*, 43–48. [CrossRef]
75. Baldas, J.; Colmanet, S.F.; Williams, G.A. Preparation and Structure of Dibromobis(N,N-diethyldithiocarbamato)-thionitrosyltechnetium(III). *Austr. J. Chem.* **1991**, *44*, 1125–1132. [CrossRef]
76. Lu, J.; Clarke, M.J. Modulation of Tc–NX (X = O or S) bonds by π-acceptor ligands. *J. Chem. Soc. Dalton Trans.* **1992**, 1243–1248. [CrossRef]
77. Abram, U.; Schulz Lang, E.; Abram, S.; Wegmann, J.; Dilworth, J.R.; Kirmse, R.; Woolins, J.D. Technetium(V) and rhenium(V) nitrido complexes with bis(diphenyl-thiophosphoryl)amide, $N(SPPh_2)^{2-}$. *J. Chem. Soc. Dalton Trans.* **1997**, 623–630. [CrossRef]
78. Hiller, W.; Hübener, R.; Lorenz, B.; Kaden, L.; Findeisen, M.; Stach, J.; Abram, U. Structural and spectroscopic studies on *mer*-dichlorotris(dimethylphenylphosphine)(thionitrosyl)technetium(I), *mer*-$[Tc(NS)Cl_2(Me_2PhP)_3]$. *Inorg. Chim. Acta* **1991**, *181*, 161–165. [CrossRef]
79. Lu, J.; Clarke, M.J. Sulfur atom transfer with reduction of a $[Tc^{VI}{\equiv}N]^{3+}$ core to a $[Tc^{I}\text{-}N{\equiv}S]^{2+}$ core. Crystal structure of mer-dichlorotris(4-picoline)(thionitrosyl)technetium. *Inorg. Chem.* **1990**, *29*, 4123–4125. [CrossRef]
80. Abram, U.; Hübener, R.; Wollert, R.; Kirmse, R.; Hiller, W. Synthesis, characterization and reactions of $[Tc(NS)X_4]^-$ complexes (X = Cl, Br, NCS). *Inorg. Chim. Acta* **1993**, *206*, 9–14. [CrossRef]
81. Dressler, K. Ultraviolett- und Schumannspektren der neutralen und ionisierten Moleküle PO, PS, NS, P_2. *Helv. Phys. Acta* **1955**, *28*, 563–590.
82. O'Hare, P.A.G. Dissociation Energies, Enthalpies of Formation, Ionization Potentials, and Dipole Moments of NS and NS^+. *J. Chem. Phys.* **1970**, *52*, 2992–2996. [CrossRef]
83. Mews, R. The Thionitrosyl Cation NS^+ as a Synthetic Reagent. *Angew. Chem. Int. Ed. Engl.* **1976**, *15*, 691–692. [CrossRef]
84. Clegg, W.; Glemser, O.; Harms, K.; Hartmann, G.; Mews, R.; Noltemeyer, M.; Sheldrick, G.M. Crystal structures of thionitrosyl hexafluoroantimonate(V) and thionitrosyl undecafluorodiantimonate(V) at 293 K and of thionitrosyl undecafluorodiantimonate(V) at 121.5 K: The effect of thermal motion on the apparent NS bond length. *Acta Cryst.* **1981**, *37b*, 548–552. [CrossRef]
85. Kaden, L.; Lorenz, B.; Kirmse, R.; Stach, J.; Abram, U. Darstellung und Charakterisierung von Thionitrosylkomplexen des Technetiums(I) und –(II). *Z. Chem.* **1985**, *25*, 29–30. [CrossRef]
86. Abram, U.; Kirmse, R.; Köhler, K.; Lorenz, B.; Kaden, L. $Tc(NX)Y_3(Me_2PhP)_2$ Complexes (X = O or S; Y = Cl or Br). Preparation, Characterization and EPR Studies. *Inorg. Chim. Acta* **1987**, *129*, 15–20. [CrossRef]
87. Nguyen, H.H.; Abram, U. Rhenium and Technetium Complexes with *N,N*-Dialkyl-*N*′-benzoylthioureas. *Inorg. Chem.* **2007**, *46*, 5310–5319. [PubMed]
88. Hayes, T.R.; Powell, A.S.; Benny, P.D. Synthesis and stability of 2 + 1 complexes of *N,N*-diethylbenzoylthiourea with $[M^I(CO)_3]^+$ (M = Re, ^{99m}Tc). *J. Coord. Chem.* **2015**, *68*, 3432–3448. [CrossRef]

89. Abram, U.; Abram, S.; Alberto, R.; Schibli, R. Ligand exchange reactions starting from $[Re(CO)_3Br_3]^{2-}$. Synthesis, characterization and structures of rhenium(I) tricarbonyl complexes with thiourea and thiourea derivatives. *Inorg. Chim. Acta* **1996**, *248*, 193–202. [CrossRef]
90. Borges, A.P.; Possato, B.; Hagenbach, A.; Machado, A.E.H.; Deflon, V.M.; Abram, U.; Maia, P.I.S. Re(V) complexes containing the phenylimido (NPh^{2-}) core and *SNS*-thiosemicarbazide ligands. *Inorg. Chim. Acta* **2021**, *516*, 120110. [CrossRef]
91. Mukiza, J.; Gerber, T.I.A.; Hosten, E.C.; Betz, R. Crystal structure of *fac*-$\kappa_{O,S}$-(Z)-1,1-diethyl-3-(hydroxido(phenyl)methylene) thiourea-($\kappa_{S'}$(Z)-1,1-diethyl-3-(hydroxido(phenyl)methylene)-thiourea)-tricarbonyl rhenium(I), $C_{27}H_{31}N_4O_5ReS_2$. *Z. Kristallogr. New Cryst. Struct.* **2015**, *230*, 50–52. [CrossRef]
92. Nguyen, H.H.; Abram, U. Rhenium and technetium complexes with tridentate S,N,O ligands derived from benzoylhydrazine. *Polyhedron* **2009**, *28*, 3945–3952. [CrossRef]
93. Salsi, F.; Portapilla, G.B.; Simon, S.; Roca Jungfer, M.; Hagenbach, A.; de Albuquerque, S.; Abram, U. Effect of Fluorination on the Structure and Anti-*Trypanosoma cruzy* Activity of Oxorhenium(V) Complexes with S,N,S-Tridentate Thiosemicarbazones and Benzoylthioureas. Synthesis and Structures of Technetium(V) Analogues. *Inorg. Chem.* **2019**, *58*, 10129–10138. [CrossRef]
94. Roca Jungfer, M.; Elsholz, L.; Abram, U. Technetium Hydrides Revisited: Syntheses, Structures, and Reactions of $[TcH_3(PPh_3)_4]$ and $[TcH(CO)_3(PPh_3)_2]$. *Organometallics* **2021**, *40*, 3095–3112. [CrossRef]
95. Kläui, W. The Coordination Chemistry and Organometallic Chemistry of Tridentate Oxygen Ligands with π-Donor Properties. *Angew. Chem. Int. Ed. Engl.* **1990**, *29*, 627–637. [CrossRef]
96. Leung, W.-H.; Zhang, Q.-F.; Yi, X.-Y. Recent developments in the coordination and organometallic chemistry of Kläui oxygen tripodal ligands. *Coord. Chem. Rev.* **2007**, *251*, 2266–2279. [CrossRef]
97. Kramer, D.J.; Davison, A.; Jones, A.G. Structural models for $[M(CO)_3(H_2O)_3]^+$ (M = Tc, Re): Fully aqueous synthesis of technetium and rhenium tricarbonyl complexes of tripodal oxygen donor ligands. *Inorg. Chim. Acta* **2001**, *312*, 215–220. [CrossRef]
98. Leung, W.-H.; Chan, E.Y.Y.; Lai, T.C.Y.; Wong, W.-T. Synthesis and reactivity of nitrido-rhenium and -osmium complexes with an oxygen tripod ligand. *J. Chem. Soc. Dalton Trans.* **2000**, 51–56. [CrossRef]
99. So, Y.-M.; Chiu, W.-H.; Cheung, W.-M.; Ng, H.-Y.; Lee, H.K.; Sung, H.H.-Y.; Williams, I.D.; Leung, W.H. Heterobimetallic rhenium nitrido complexes containing the Kläui tripodal ligand $[Co(\eta^5\text{-}C_5H_5)\{P(O)(OEt)_2\}_3]^-$. *Dalton Trans.* **2015**, *44*, 5479–5487. [CrossRef]
100. Banberry, H.J.; Hussain, W.; Evans, I.G.; Hamor, T.A.; Jones, C.J.; McCleverty, J.A.; Schulte, H.-J.; Engles, B.; Kläui, W. The syntheses of high oxidation state metal complexes containing the tripodal ligand $[(\eta^5\text{-}C_5H_5)Co\{P(OMe)_2(O)\}_3]^-$ and the X-ray crystal structure of $[(\eta^5\text{-}C_5H_5)Co\{P(OMe)_2(O)\}_3\ ReO_3]$. *Polyhedron* **1990**, *9*, 2549–2551. [CrossRef]
101. Dyckhoff, B.; Schulte, H.-J.; Englert, U.; Spaniol, T.P.; Kläui, W.; Schubiger, P.A. Rhenium-Komplexe von Sauerstoffchelatliganden: Ein Weg zu neuen Radiopharmaka? *Z. Anorg. Allg. Chem.* **1992**, *614*, 131–141. [CrossRef]
102. Abram, U.; Abram, S. Synthese und Charakterisierung neuartiger Technetiumkomplexe mit 1,1-disubstituierten Benzoylthioharnstoffen. *Z. Chem.* **1983**, *23*, 228. [CrossRef]
103. Sullivan, B.P.; Brewer, J.C.; Gray, H.B.; Linebarrier, D.; Mayer, J.M. Nitrido and Oxo Complexes of Rhenium(V). *Inorg. Synth.* **1992**, *29*, 146–150.
104. Kaden, L.; Lorenz, B.; Schmidt, K.; Sprinz, H.; Wahren, M. Nitridokomplexe des Technetium(V). *Isotopenpraxis* **1981**, *17*, 174–175.
105. Baldas, J.; Boas, J.F.; Bonnyman, J.; Williams, G.A. Studies of technetium complexes. Part 6. The preparation, characterisation, and electron spin resonance spectra of salts of tetrachloro- and tetrabromonitridotechnetate(VI): Crystal structure of tetraphenylarsonium tetrachloronitridotechnetate(VI). *J. Chem. Soc. Dalton Trans.* **1984**, *11*, 2395–2400. [CrossRef]
106. Abram, U.; Braun, M.; Abram, S.; Kirmse, R.; Voigt, A. $[NBu_4][ReNCl_4]$: Facile synthesis, structure, electron paramagnetic resonance spectroscopy and reactions. *J. Chem. Soc. Dalton Trans.* **1998**, *2*, 231–238. [CrossRef]
107. Grunwald, A.C. Metal Complexes with Tripodal and Chelating Thiourea Ligands towards Nuclear Medical Imaging. Doctoral Thesis, Freie Universität Berlin, Berlin, Germany, 2020. Available online: https://refubium.fu-berlin.de/handle/fub188/30387 (accessed on 1 July 2024).
108. Nowak, D. Thionitrosylkomplexe des Rheniums und Technetiums. Doctoral Thesis, Freie Universität Berlin, Berlin, Germany, 2022. Available online: https://refubium.fu-berlin.de/handle/fub188/36899 (accessed on 1 July 2024).
109. Kleinpeter, E.; Beyer, L. ^{1}H-NMR-Untersuchung der behinderten Rotation um die C-N-Bindung in 1,1′-Diäthyl-3-benzoylharnstoff-Derivaten. *J. Prakt. Chem.* **1975**, *317*, 938–942. [CrossRef]
110. Stoll, S.; Schweiger, A. EasySpin, a comprehensive software package for spectral simulation and analysis in EPR. *J. Magn. Res.* **2006**, *178*, 42–55. [CrossRef] [PubMed]
111. *MATLAB Version: 9.13.0 (R2022b)*; The MathWorks Inc.: Natick, MA, USA, 2022.
112. Sheldrick, G. *SADABS, vers. 2014/5*; University of Göttingen: Göttingen, Germany, 2014.
113. Coppens, P. The Evaluation of Absorption and Extinction in Single-Crystal Structure Analysis. In *Crystallographic Computing*; Muksgaard: Copenhagen, Denmark, 1979.
114. Sheldrick, G.M. A short history of SHELX. *Acta Crystallogr.* **2008**, *A64*, 112–122. [CrossRef] [PubMed]
115. Sheldrick, G.M. Crystal structure refinement with SHELXL. *Acta Crystallogr.* **2015**, *C71*, 3–8.
116. Farrugia, L.J. WinGX and ORTEP for Windows: An update. *J. Appl. Cryst.* **2012**, *45*, 849–854. [CrossRef]

117. Dolomanov, O.V.; Bourhis, L.J.; Gildea, R.J.; Howard, J.A.; Puschmann, H. OLEX2: A complete structure solution, refinement and analysis program. *J. Appl. Crystallogr.* **2009**, *42*, 339–341. [CrossRef]
118. Putz, H.; Brandenburg, K. *Diamond—Crystal and Molecular Structure Visualization*; Vers. 4.6.8.; Crystal Impact: Bonn, Germany, 2022.